Stator optimization of six-phase claw-pole alternators using asymmetric winding arrangements

S. Schulte, C. Kaehler, C. Schlensok and G. Henneberger
Institute of Electrical Machines, RWTH Aachen University, Aachen, Germany

Abstract

Purpose – To present a new approach for improvement and optimization of synchronous claw-pole alternators without changing the general machine design.

Design/methodology/approach – Various changes on the magnetically relevant parts of the machine design have been discussed formerly to achieve improved electromagnetic and acoustic behavior. The electrical part of the machine is considered in this paper, varying the stator winding arrangement to achieve optimized behavior.

Findings – Provides information about motivation and the methodology of the optimization process. Presents the entire analysis, covering idea, technical and computational implementation as well as verification.

Research limitations/implications – It describes a method based on the utilization of specific, partly self-generated software, which perhaps limits its usefulness if mentioned tools are unavailable. However, the presented basic method is to be used generally.

Originality/value – This paper presents a promising approach to further optimize the design of synchronous claw-pole alternators without major changes in the machine design.

Keywords Finite element analysis, Optimization techniques, Alternating current, Electric machines

Paper type Technical paper

Introduction

The design of common three-phase claw-pole alternators basically consists of the DC excited rotor with characteristic claw fingers and the stator, equipped with a two-layer three-phase winding. The alignment and the phasor diagram of the stator windings are shown in Figure 1(a) and (b). The expansion of the winding system to six-phases reduces DC-link current ripples of the rectifier and therefore expands the duty cycle of the rectifier components. Besides current ripple reduction, the utilization of six-phases reduces demands on ampacity of components of each phase. However, acoustic advantages will come along as a benefit.

Basic structure

The considered six-phase winding consists of two separated parallel three-phase windings (Figure 2(a) and (b)). The stator of the six-phase machine consists of 72 slots, resulting in a slot pitch of the stator teeth of $\gamma = 5°$. Owing to cost minimization the

This paper is dedicated to Prof. Gerhard Henneberger, who is released into his well deserved retirement with gratitude and appreciation for his meritorious scientific work.

COMPEL: The International Journal for Computation and Mathematics in Electrical and Electronic Engineering
Vol. 25 No. 2, 2006
pp. 389-398

0332-1649
DOI 10.1108/03321640610649069

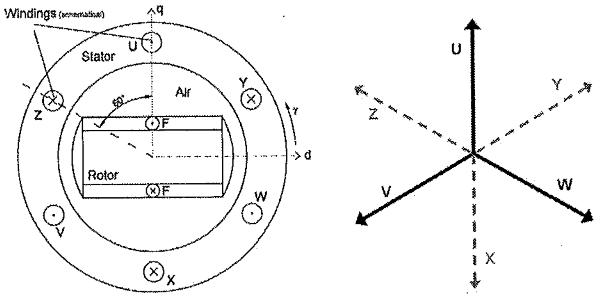

(a)
3-phase salient-sole synchronous machine

(b)
Accordant phasor orientation (3-ph)

Figure 1.

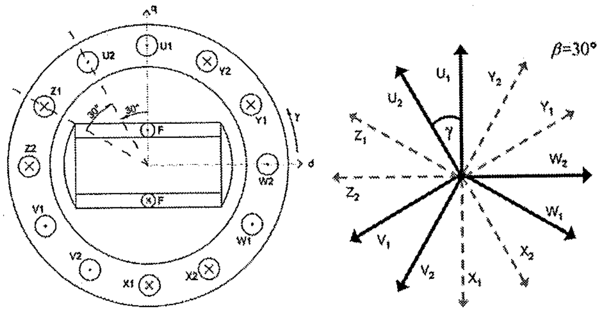

(a)
Expansion up to 6 stator phases

(b)
Accordant phasor orientation (6-ph)

Figure 2.

number of stator slots is fixed and not part of investigations. Moreover, the winding distribution based on the slot number is subject of this paper.

Both separate three-phase windings are shifted n-times the slot pitch $\beta = n\gamma$ (Figures 3(a) and (b) and 4(a) and (b)) to each other. The obvious arrangement of stator phases (Figure 2(a) and (b)) does not necessarily result in the best possible solution due to electric and magnetic requirements as well as to acoustic demands.

Asymmetric winding arrangements lead to both an asymmetric flux distribution and local saturation discrepancies in the stator. The determination of appropriate winding configurations (Figures 3(a) and (b) and 4(a) and (b)) is subject to computational analysis.

Approach

Electric optimization

Preliminary studies. In a first step of the optimization process, a set of different winding arrangements is selected with respect to given electric requirements.

Analytical means (Matlab/Simulink, www.mathworks.com) as well as simulation tools (Simplorer, Ansoft Inc., www.ansoft.com) are utilized for this purpose.

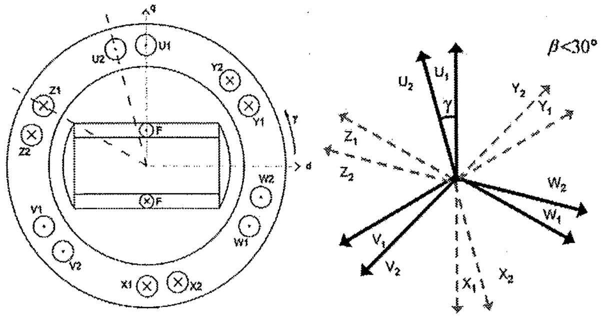

(a) Varied stator arrangement

(b) Accordant phasor orientation

Figure 3.

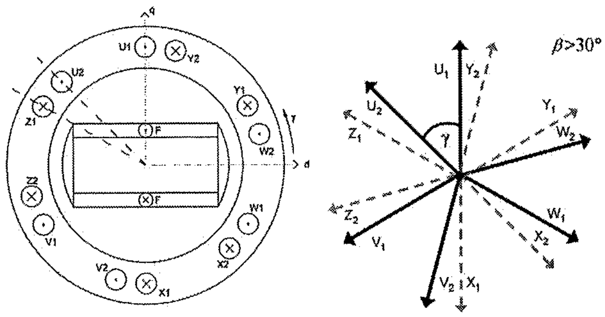

(a) Varied stator arrangement

(b) Accordant phasor orientation

Figure 4.

At this early stage of design, phase currents of the alternator are assumed to be sinusoidal shaped for simplification reasons. This approximation is considered reasonable for the entire speed and excitation ranges. Phase current equations for both winding systems (index 1 and 2 in Figures 2-4) are based on equations (1) and (2). The implementation in Matlab (Matlab/Simulink, www.mathworks.com) is brief (shown in Figure 5, top).

$$i_{1k+1} = \hat{I}\sin\left(\omega t + \frac{2k\pi}{3}\right) \quad (1)$$

$$i_{2k+1} = \hat{I}\sin\left(\omega t + \beta + \frac{2k\pi}{3}\right) \quad (2)$$

with the displacement angle β, $k = 0, 1, 2$.

The influence of inductive coupling of other phases and the synchronous generated voltage is not considered at this stage. This approximation is reasonable for both considered speed and excitation ranges entirely.

The accordant DC-link current (Figure 5, bottom) ensues to:

$$i_{\mathrm{DC-Link}} = \sum_{1}^{2} |i_{\mathrm{UVW}}(t)| \tag{3}$$

At $\beta = 0$ the machine behaves as a double two-layer three-phase machine concerning current magnitude and frequency. If the angular displacement amounts $\beta = 30°$, the DC-link current is of double frequency compared to the three-phase case. All other winding displacement-compositions $0° < \beta < 30°$ require Fourier analysis for the determination of the fundamental frequency and higher harmonics.

Owing to counteracting inductive influences of the phase currents, peak values of both phase current and DC-link current vary with β.

It turns out, that a significant drop of current peak values ($\approx$ 5percent) has minor influence on the accodant RMS value, as Figure 6 shows.

Since a reduction of peak values is desirable from the electrical point of view, winding displacements are most reasonable in the range of $\beta_{\min} \leq 30° \leq \beta_{\max}$, stating the applicable symmetry range at the same time.

Detailed curve sketching. Other than for the simplified preliminary studies, mainly covering the macro-structural correlation of the winding system with the environmental vehicle power supply system, the curve sketching covers the internal machine behavior. For the detailed characteristic analysis, waveform simplifications are no longer feasible. Mutual inductive influences of the stator-phase currents, varying with the displacement angle β, effect the shape of the phase currents, i.e. the magnitude and the frequency. Therefore, the harmonic analysis requires an authentic description of the current waveforms, taking particular winding arrangements into account.

The entire set of differential equations, describing the full machine behavior, contains currents (equations (4) and (5)), flux linkage (equation (6)), position dependent

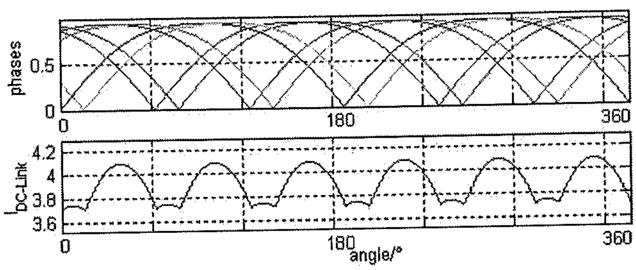

Figure 5.
$I_{1,2k}$ (top), $I_{\text{DC-link}}$ (bottom), 45° displaced

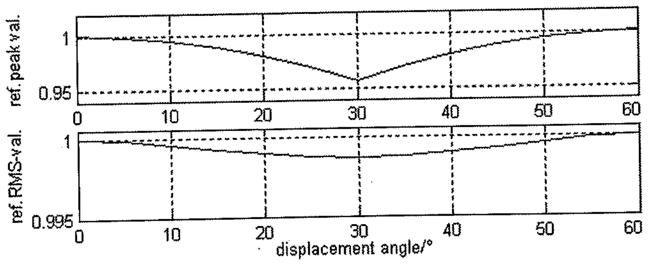

Figure 6.
Referred peak (top), RMS (bottom) values of $I_{1,2k}$, symmetry range of $0° \leq \beta \leq 60°$ displacement

inductances (equation (7)) and motion (equations (8) and (9)) must be set up to describe the machine behavior entirely.

Different from the simplified pre-investigations, being subject to Matlab simulations, the entire differential equation set, stating a behavioral machine model is released in VHDL-AMS (1993). VHDL-AMS is a standardized hardware description language for modeling of analog and mixed signal devices.

$$\left.\begin{aligned} i_{U1} &= \frac{\psi_{U1}}{L_{U1}} - i_{V1}\frac{L_{U1V1}}{L_{U1}} - i_{W1}\frac{L_{U1W1}}{L_{U1}} - i_{U2}\frac{L_{U1U2}}{L_{U1}} - i_{V2}\frac{L_{U1V2}}{L_{U1}} - i_{W2}\frac{L_{U1W2}}{L_{U1}} - i_{F}\frac{L_{U1F}}{L_{U1}} \\ i_{U2} &= \frac{\psi_{U2}}{L_{U2}} - i_{U1}\frac{L_{U1U2}}{L_{U2}} - i_{V1}\frac{L_{V1U2}}{L_{U2}} - i_{W1}\frac{L_{W1U2}}{L_{U2}} - i_{V2}\frac{L_{U2V2}}{L_{U2}} - i_{W2}\frac{L_{U2W2}}{L_{U2}} - i_{F}\frac{L_{U2F}}{L_{U2}} \end{aligned}\right\} \tag{4}$$

$$i_F = \frac{\psi_F}{L_F} - i_{U1}\frac{L_{U1F}}{L_F} - i_{V1}\frac{L_{V1F}}{L_F} - i_{W1}\frac{L_{W1F}}{L_F} - i_{U2}\frac{L_{U2F}}{L_F} - i_{V2}\frac{L_{V2F}}{L_F} - i_{W2}\frac{L_{W2F}}{L_F} \tag{5}$$

$$\left.\begin{aligned} \psi_{U1} &= \int (u_{U1} - i_{U1}R_{U1})\mathrm{d}t \Leftrightarrow u_{U1} = i_{U1}R_{U1} + \frac{\mathrm{d}\psi_{U1}}{\mathrm{d}t} \\ \psi_{U2} &= \int (u_{U2} - i_{U2}R_{U2})\mathrm{d}t \Leftrightarrow u_{U2} = i_{U2}R_{U2} + \frac{\mathrm{d}\psi_{U2}}{\mathrm{d}t} \end{aligned}\right\} \tag{6}$$

analogous for phase V1, V2, W1, W2 and excitation F.

$$\left.\begin{aligned} L_{U1F} &= L_{FS}\cos\left(\gamma + \frac{\pi}{12} - \frac{2k\pi}{3}\right), \quad k = 0 \\ L_{U2F} &= L_{FS}\cos\left(\gamma - \frac{\pi}{12} - \frac{2k\pi}{3}\right), \quad k = 0 \end{aligned}\right\} \tag{7}$$

analogous for phase V1, V2 ($k = 1$) and W1, W2 ($k = 2$).

$$\gamma = \gamma_0 + \int \omega\,\mathrm{d}t \Rightarrow \gamma - \gamma_0 + \int \omega\,\mathrm{d}t = 0 \tag{8}$$

$$\dot{\omega} = \frac{1}{J}(M_i - M_W) \tag{9}$$

The VHDL-AMS six-phase claw-pole alternator machine model is simulated in a simplified vehicle power supply network, shown in Figure 7.

This simulation environment contains the external excitation circuit, an uncontrolled B12 rectifier bridge, the battery and the simulated load behavior of other components, and is entirely implemented and embedded in Simplorer (Simplorer, Ansoft Inc., www.ansoft.com).

VHDL-AMS was originally developed for the modeling of integrated circuits. It turned out to be a mighty and powerful means for the modeling of almost any kind of

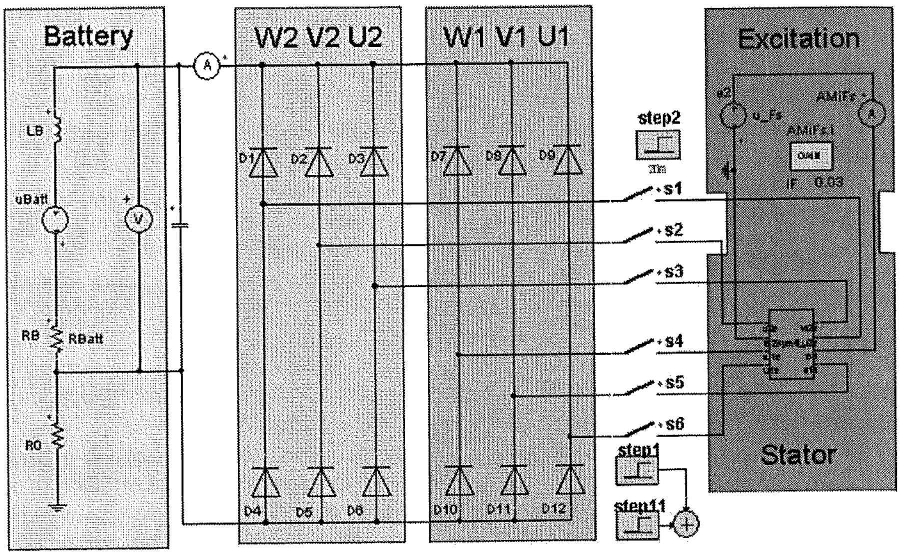

Figure 7.
Simplorer simulation sheet, VHDL machine model

electric and electromagnetic component (mechanical, fluid and thermal models are also possible), so that the AMS extension (*i*MOOSE – innovative Modern Object-Oriented Solver Environment, www.imoose.de) has been added to the IEEE standard.

The vehicle-power supply-simulation of the VHDL-AMS implemented alternator is used to check on sufficient performance of power demands such as current limitation or torque exertion for verification purposes.

The combination of the analytical equation set up in the VHDL-AMS machine model and the simulation in Simplorer allows for comfortable and unrestricted parameter access. Any variable or parameter is accessible, can be plotted (Figure 8), modified, or adapted for optimization purposes in further simulations. Figure 8 shows

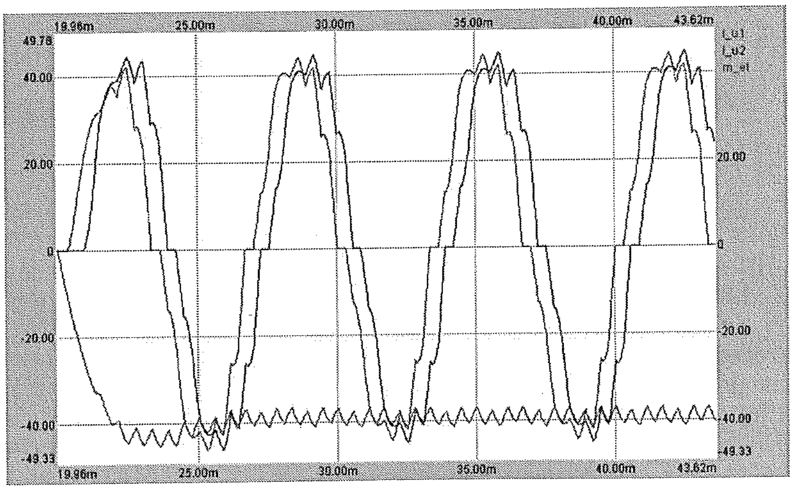

Figure 8.
Simplorer plot of currents i_{U1}, i_{U2} and torque M_{el} vs time

a plot of two stator currents i_{U1}, i_{U2} and torque M_{el} vs time as an example for graphical parameter output.

For the considered machine design: mutual angular displacement of both stator-winding systems are modified by simple parameter variation. The stator winding arrangement is varied by adapting the mutual inductances between stator phases of both systems number 1 and 2, as well as the mutual inductances between stator and rotor. Particular steps of integer pole pitch widths are based on this displacement (steps of 5° for the considered alternator constructed with 72 stator slots).

The variation of the number of windings or the winding profile as such is also conceivable, affecting internal parameters, such as the flux or the magnetomotive force.

Besides verification purposes, analysis opportunities are provided. Each variable of the analytically implemented VHDL-AMS model can be saved for post-processing means.

The VHDL-AMS machine-model implementation provides saving of results of arbitrary variables in ASCII files – here the stator currents and torque characteristics. The ASCII files (Figure 9) contain equidistant time base and accordant current and torque values column wise, tab separated each.

The choice of using a plain text format for the simulation result target files offers universal utilization opportunities for further processing, largely independent from manufacturer specific data formats.

The described simulation results in ASCII representation state the input files for the harmonic analysis of the considered detailed investigation. Therefore, the simulation results are imported into the Matlab workspace with no more file format adaptation needed. Workspace content adaptation merely affects required cut outs of transient phenomena.

Torque and current characteristics – the latter to be squared for stator force estimation – are processed using a Matlab implemented Fourier analysis routine.

This routine auto detects an entire cycle of the characteristic to be analyzed; solely the accordant resolution needs to be defined manually. Appliance of the analytically implemented Fourier analysis leads to frequency results showing contained fundamental wave and harmonics as exemplarily illustrated for stator current i_{U1} and torque M_{el} in Figures 10 and 11.

simudata.txt - Notepad

File Edit Format View Help

1	-77.0798	38.17390	38.9059 6	0.090897
2	-76.4829	37.49130	38.9917 6	0.180895
3	-75.8741	36.78010	39.094 6	0.270892
4	-75.2565	36.04140	39.2151 6	0.360889
5	-74.6295	35.27440	39.3551 6	0.450887
6	-73.9924	34.47800	39.5144 6	0.540884
7	-73.3445	33.65150	39.6931 6	0.630881
8	-72.6849	32.79360	39.8913 6	0.720879
9	-72.0128	31.90350	40.1094 6	0.810876
10	-71.3273	30.98000	40.3473 6	0.900873
11	-70.6276	30.02220	40.6054 6	0.990871
12	-69.9128	29.02910	40.8837 6	1.080870
13	-69.1820	27.99970	41.1823 6	1.170870
14	-68.4343	26.93300	41.5014 6	1.260860
15	-67.6689	25.82790	41.841 6	1.350860
16	-66.8849	24.68360	42.2013 6	1.440860
17	-66.0813	23.49900	42.5823 6	1.530850
18	-65.2572	22.27330	42.9839 6	1.620850
19	-64.4119	21.00570	43.4062 6	1.710850
20	-63.5443	19.69530	43.8491 6	1.800850
21	-62.6537	18.34130	44.3124 6	1.890840
22	-61.7392	16.94300	44.7962 6	1.980840

Figure 9.
Simulation data in ASCII file

Magnetic optimization

The resulting configuration of the electrical pre-designing process does not necessarily need to state a reasonable choice from the magnetic point of view, so that reasonable winding arrangements resulting from the analytical optimization process need to be evaluated due to their magnetic behavior using numerical methods.

Although current peak values are significantly decreased by duplicating the number of phases, the angular displacement of both winding systems may lead to local flux superelevation, based on disadvantageous winding correlation.

Besides superelevation, asymmetric saturation in stator teeth and yoke may occur for the considered machine design, based on parasitic flux distribution, ensuing in unwanted and parasitic effects such as torque ripples, noise or local eddy current accumulation.

The resulting configuration of the electrical optimization process does not necessarily need to state a reasonable choice from the magnetic point of view.

The given machine type, featuring variable stator winding arrangements, results in an accordant asymmetric flux distribution. This may lead to desirable benefits, such as a reduction of noise and on the other hand to unwanted and parasitic effects.

Therefore, numerical methods, such as FE simulations, are applied to double check both on proper magnetic design (Figure 12) as well as on correct results of the analytical calculations of electrical and mechanical values.

The given example of a six-phase claw-pole alternator is magnetically designed using ANSYS (ANSYS Inc., www.ansys.com) for modeling and meshing and a self-developed object-oriented solver environment *i*MOOSE (*i*MOOSE – innovative

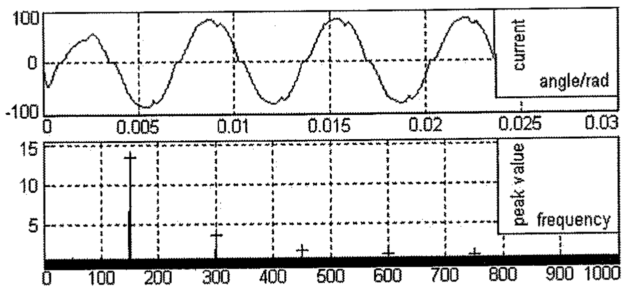

Figure 10.
Current i_{U1} waveform (top), FFT (bottom)

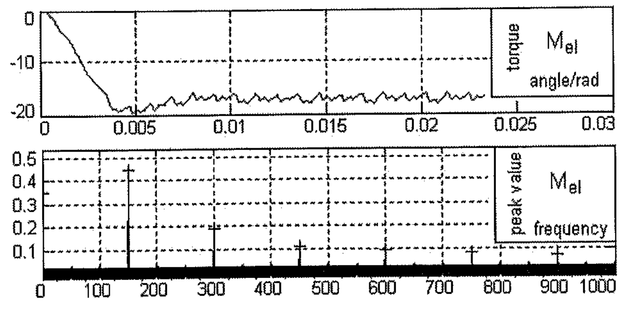

Figure 11.
Torque M characteristic (top), FFT (bottom)

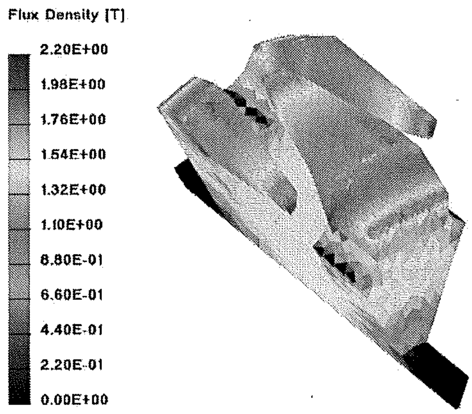

Figure 12.
Flux density in rotor out of FE simulation

Modern Object-Oriented Solver Environment, www.imoose.de) with static and transient 3D solvers for computation, post-processing and visualization. The *i*MOOSE package is partly open source and is subject to further development (Figure 13).

Conclusion

The variation of the stator winding arrangement of a six-phase claw-pole alternator enables opportunities for electric, magnetic, and acoustic optimization. A method to design and optimize the stator arrangement of a six-phase claw-pole alternator is presented.

At first this scheme consists of analytical pre-design for a pre-selection of reasonable stator-winding configurations. SPICE-oriented simulation concepts determine the real machine behavior running in a vehicle power supply network model, with regular duty cycles as well as fault scenarios being applicable.

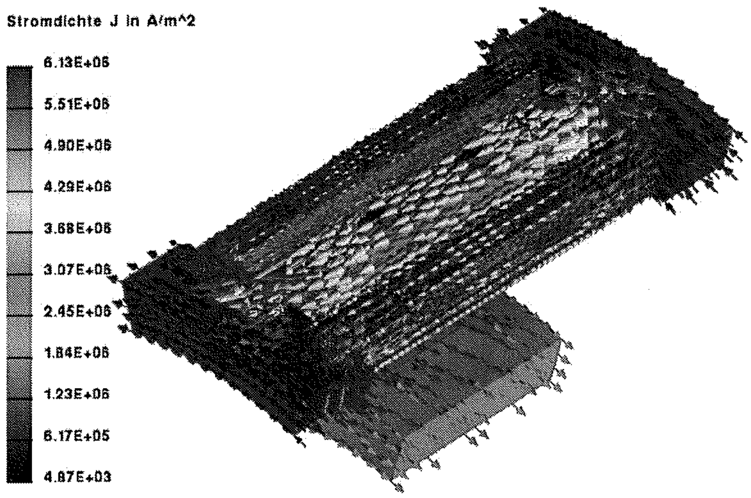

Figure 13.
Current density in stator and field windings

Electromagnetic design as well as a verification of the pre-design iteration-step is performed using FE simulation. The performed FE analysis of the machine model enables powerful post-processing opportunities, such as investigations on force, acoustics and structure-dynamics.

Reference

VHDL-AMS (1993), "VHDL-AMS: very high speed hardware description language – analog and mixed signals", IEEE 1076.1-1993.

Further reading

Kaehler, C. and Henneberger, G. (2000), "Calculation of the differences in the acoustical behaviour of a claw-pole alternator when connected in delta and star", paper presented at Second International Seminar on Vibrations and Acoustic Noise in Electric Machinery, VANEM.

Kaehler, C. and Henneberger, G. (2001), "Calculation of the mechanical and acoustic behaviour of a claw-pole alternator in double and single star connection", paper presented at Fourth International Symposium on Advanced Electromechanical Motion Systems, Electromotion.

Corresponding author

S. Schulte can be contacted at: stephan.schulte@iem.rwth-aachen.de